❐   109

Speed-planning algorithm and super twisting control for autonomous vehicle steering system

Sofiane Bacha[1], Ramzi Saadi[1], Mohamed-Yacine Ayad[2], Abdennacer Aboubou[1]
[1]Department of Electrical Engineering, Faculty of Technology, Mohamed Khider University, Biskra, Algeria
[2]Industrial Hybrid Vehicle Applications, France

Article Info	ABSTRACT
	Autonomous vehicle field has seen much development in recent years, especially with the appearance of new efficient control techniques focusing on longitudinal and lateral direction in order to follow a specified trajectory or path. This paper proposes a new systematic control technique to simultaneously generate a suitable speed profile and control the vehicle lateral motion through a predetermined path that considers different driving scenarios representing real-world driving. First, an extended-kinematic model for an autonomous vehicle is designed based on side-slip angle estimation. Then, the proposed technique uses a relationship between lateral error, heading error, and vehicle velocity to generate a suitable steering angle based on super twisting mode control. Second, a speed-planning algorithm is developed to control vehicle velocity. The algorithm uses a strategy for sharp curve identification; then it generates an adequate speed profile depending on the dynamic characteristics of these curves to ensure smooth motion of the vehicle through the whole trajectory. The obtained results from using a speed-planning algorithm with a super twisting controller prove the high performance of this control technique in terms of decreasing errors and respecting passenger comfort.

Corresponding Author:

Sofiane Bacha
Energy Systems Modeling Laboratory, Department of Electrical Engineering, Faculty of Technology
Mohamed Khider University
Biskra, Algeria
Email: sofiane.bacha@hotmail.fr

1. INTRODUCTION

Autonomous ground vehicles, as a crucial part of the urban transportation system, have become a major axis of research in the automotive industry field. Six standards of autonomy were introduced, from "no autonomous" to "full autonomous" [1]. an automated vehicle system is classified as fully autonomous if there is no human intervention. This type of vehicles has proved to be an efficient transportation way and it is getting more interest than ever before in our society. Currently, autonomous vehicles can only perform the basic operations. Broadly speaking, the driving task includes three sub-tasks [2]: i) sensing and perception; ii) planning and decision; and iii) vehicle control.

In real driving scenarios, lateral and longitudinal controllers are the two basic requirements for vehicle navigation. Lateral control refers to the task of steering and navigating laterally on the road. While longitudinal control is the task where we control the velocity of the car along the roadway, through actions like breaking or acceleration. Different modelling techniques have been proposed for trajectory-tracking field. Many of them are based on kinematic or dynamic vehicle models [3], while others use an extended-

kinematic model [4]–[6]. This last considers the effects of contact forces as disturbances of the model, changing the angular and lateral evolution of the vehicle.

Various techniques have also been developed to control these systems; one interesting approach was provided in [7], which presented a robust lateral torque control function based on Lyapunov method and gain scheduling technique for lateral tracking to ensure both robustness and stability. Mohammadzadeh and Taghavifar [8] proposed a robust fuzzy approach for autonomous vehicle path-following is proposed. The system performance was verified in a double-lane-change case under different types of disturbances. Ji *et al.* [9] used a new control technique, based on coordinate control path-following and yaw moment control, to improve the pursuit accuracy and vehicle stability. A linear time-varying predictive control was used first to generate an accurate steering angle for the front-wheel, then the yaw moment is distributed with vehicle torque requirement. Akermi *et al.* [10] used a novel sliding-mode in path-following task for autonomous vehicle. They used a fuzzy system for sliding-mode gain automatic adjustment, a disturbance observer for mismatched disturbances estimation and a radial basis function neural networks for uncertainties assessing. Guo *et al.* [11] proposed a robust H-infinity fault tolerant steering system for autonomous vehicles to improve lateral driving performance while dealing with actuator faults and parameter uncertainties. Baker and Ghadi [12] proposed a fuzzy controller to control an autonomous mobile robot obstacle avoidance by using an adaptive inference engine, fuzzing and defuzzification engine. Shamsuddin *et al.* [13] reviewed the techniques used in path following and trajectory tracking for autonomous vehicles over recent years, highlighting the advantages and capabilities of each technique.

Most of these mentioned researches dealt with controlling the vehicle lateral motion relatively to the desired path and increasing the system robustness against disturbances. However, there are some works focused on vehicle longitudinal motion by integrating velocity control. Serna and Ruichek [14] developed a dynamic speed adaption algorithm where the vehicle speed is adapted based on road speed limits and path information. In the DARPA grand-challenge (2005), stanley robot [15] used a speed recommender, health monitor, and trajectory planner, to design a powerful system capable of navigating in off-road environments with a high-speed profile. Taheri-Kalani and Zarei [16] designed a sensorless trajectory tracking technique by using a nonlinear observer to neglect velocity sensor and adaptive model reference control to design a dynamic controller. Lee and Prabhuswamy [17] developed an algorithm to determine the adequate speed profile based on speed-limit changes and trajectory curves. The generated speed reference is integrated with conventional adaptive cruise controller to control the vehicle speed. Deng *et al.* [18] introduced in their research a driver factor, which is acquired from the ratio of driver's desired speed with the theoretical curve's speed. This factor is integrated with previous vehicle-road interaction model.

The main contribution in this paper includes a performance improvement of the autonomous vehicle steering system by combining a lateral super twisting controller with an algorithm of speed planning. Based on extended-kinematic model, a super twisting controller is designed to control the vehicle lateral position by generating a reference steering command for the steering actuator, ensuring vehicle navigation within the limited boundaries. A curve identification technique is then used to automatically extract the parameters of trajectory curvatures from geographic information. The obtained data is used in combination with road friction factor and super-elevation angle to generate an adequate speed profile for vehicle motion.

The organization of the paper is as follows: section 2 presents a mathematical description of the extended-kinematic model. Section 3 provides the super twisting lateral controller design. Section 4 describes the identification of trajectory curvatures and the algorithm used to generate the speed profile. Section 5 details the designed controller performance through simulation results with and without using speed planning algorithm. The last section contains conclusions.

2. AUTONOMOUS VEHICLE MODELING

This section addresses autonomous vehicle modeling task. The vehicle is modelled as a single rigid body and its evolution can be related to that of a bicycle. Just the front-wheel is steerable.

2.1. Extended kinematic model

The kinematic model detailed in [19] described the vehicle evolution under rolling without slipping assumption [20]. In the context of trajectory-tracking, where speed changes are relatively limited, longitudinal sliding is not considered. The main effect changing the vehicle movement is the lateral sliding creating a slip angles in the wheels of the vehicle, β_F for the front-wheel and β_R for the rear-wheel [21]. Hence, the extended-kinematic model for the vehicle in absolute coordinates can be written as (1) [22]:

$$\begin{bmatrix} \dot{x}_r \\ \dot{y}_r \\ \dot{\theta}_r \end{bmatrix} = v \cdot \begin{bmatrix} \cos(\theta_r + \beta_R) \\ \sin(\theta_r + \beta_R) \\ \cos(\beta_R) \cdot \frac{\tan(\psi_r + \beta_F) - \tan(\beta_R)}{l} \end{bmatrix} \tag{1}$$

where x_r and y_r are the vehicle actual coordinates, θ_r is the vehicle orientation, v is the vehicle linear velocity, l is the vehicle length, and ψ_r is the front steering angle.

2.2. Sideslip angle estimation

We want to obtain values for the two side-slip angles (β_F, β_R). The direct measurement of these angles is hardly feasible. Therefore, an indirect estimate is necessary to be carried out. The general principle of the designed observer is presented in [5]. It is based on using measurements from the real process from which the measured variable $X(y_r, \theta_r)$ is deduced. This model allows to calculate an estimated evolution of the variable $\hat{X}(\hat{y}_r, \hat{\theta}_r)$. The measured system state, composed of lateral and angular position, is deduced (2):

$$\dot{X} = \begin{bmatrix} v \cdot sin(\theta_r + \beta_R) \\ v \cdot \cos(\beta_R) \cdot \frac{\tan(\psi_r + \beta_F) - \tan(\beta_R)}{l} \end{bmatrix} \tag{2}$$

The state equation of the system observed is therefore (3):

$$\dot{\hat{X}} = \begin{bmatrix} v \cdot sin(\widehat{\theta_r} + \widehat{\beta_R}) \\ v \cdot \cos(\widehat{\beta_R}) \cdot \frac{\tan(\psi_r + \widehat{\beta_F}) - \tan(\widehat{\beta_R})}{l} \end{bmatrix} \tag{3}$$

As side-slip angles are limited to a few degrees, the observed state model can be linearized under small drift angles assumption. The nonlinear state model therefore becomes linear (4):

$$\dot{\hat{X}} = \begin{bmatrix} v \cdot sin(\widehat{\theta_r}) \\ v \cdot \frac{\tan(\psi_r)}{l} \end{bmatrix} + \begin{bmatrix} 0 & v \cdot cos(\widehat{\theta_r}) \\ \frac{v}{l.cos^2\psi_r} & -\frac{v}{l} \end{bmatrix} \cdot \begin{bmatrix} \widehat{\beta_F} \\ \widehat{\beta_R} \end{bmatrix} \tag{4}$$

Knowing that X is a measure of the state, the observation error is then completely defined as (5):

$$e_{obs} = \hat{X} - X \tag{5}$$

The error dynamics is imposed according to the relation (6):

$$\dot{e}_{obs} = M \cdot e_{obs} \tag{6}$$

The choice of the matrix M Hurwitz allows to ensure the observation error convergence towards zero, and therefore the estimated state convergence towards the measured state [23]. The estimated side-slip angles are therefore deduced verifying the relation in (7).

$$\begin{bmatrix} \widehat{\beta_F} \\ \widehat{\beta_R} \end{bmatrix} = \begin{bmatrix} 0 & v \cdot cos(\widehat{\theta_r}) \\ \frac{v}{l.cos^2\psi_r} & -\frac{v}{l} \end{bmatrix}^{-1} \cdot \left[M \cdot e_{obs} - \begin{bmatrix} v \cdot sin(\widehat{\theta_r}) \\ v \cdot \frac{\tan(\psi_r)}{l} \end{bmatrix} + \dot{X} \right] \tag{7}$$

3.   CONTROL LAW DESIGN

In the previous section, a model for autonomous vehicle was introduced. To enable the vehicle to accurately follow a continuous curvature path, a control technique must be developed, where the variables that comprise vehicle posture will be controlled (x_r, y_r, θ_r).

3.1. Path following

Path-following strategy deals with controlling the vehicle lateral deviation around the reference path, and ensuring smooth tracking while maintaining appropriate passenger comfort. The error calculation is used to compute the errors in angle θ_e and distance y_e. By defining a point on one look-ahead distance L_a from the vehicle rear-wheel (Figure 1), the error vector can be defined as (8):

$$\begin{bmatrix} y_e \\ \theta_e \end{bmatrix} = \begin{bmatrix} -\sin(\theta_d) & \cos(\theta_d) & 0 \\ 0 & 0 & 1 \end{bmatrix} \begin{bmatrix} x_r - x_d + L_a \cdot \cos(\theta_r) \\ y_r - y_d + L_a \cdot \sin(\theta_r) \\ \theta_r - \theta_d \end{bmatrix} \tag{8}$$

Here, (x_d, y_d, θ_d) denotes the desired vehicle pose, and (x_r, y_r, θ_r) is the actual vehicle pose. By considering the side-slip angles (β_F, β_R) the new error vector, named (y_{e1}, θ_{e1}), becomes (9):

$$\begin{bmatrix} y_{e1} \\ \theta_{e1} \end{bmatrix} = \begin{bmatrix} -\sin(\theta_d) & \cos(\theta_d) & 0 \\ 0 & 0 & 1 \end{bmatrix} \begin{bmatrix} x_r - x_d + L_a \cdot \cos(\theta_r + \beta_R) \\ y_r - y_d + L_a \cdot \sin(\theta_r + \beta_R) \\ \theta_r + \beta_R - \theta_d \end{bmatrix} \tag{9}$$

Its corresponding derivative (10):

$$\begin{bmatrix} \dot{y}_{e1} \\ \dot{\theta}_{e1} \end{bmatrix} = \begin{bmatrix} v \cdot \sin(\theta_{e1}) + L_a \cdot v \cdot \cos(\beta_R) \cdot \frac{\tan(\psi_r + \beta_F) - \tan(\beta_R)}{l} \cdot \cos(\theta_{e1}) \\ v \cdot \cos(\beta_R) \cdot \frac{\tan(\psi_r + \beta_F) - \tan(\beta_R)}{l} \end{bmatrix} \tag{10}$$

To avoid cutting edges during vehicle navigation, a designed algorithm for look-ahead distance selection is considered. In this paper, the look-ahead distance value is set to be between $0.5\ m$ and $10\ m$ within a path curvature range, κ, of 0.01 to 0.05, as shown in (11):

$$L_a = \begin{cases} 10 & \kappa < 0.01 \\ -237.5 \cdot \kappa + 12.375 & 0.01 < \kappa < 0.05 \\ 0.5 & 0.05 < \kappa \end{cases} \tag{11}$$
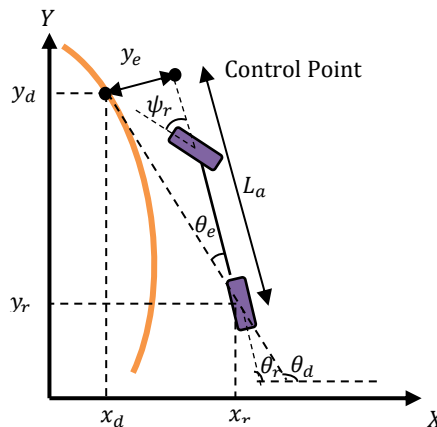

Figure 1. Lateral control parameters with look ahead distance

3.2. Super twisting control

A robust lateral controller should be designed so that the vehicle can correctly pursuit the desired path. In this paper, super twisting mode is considered. The super twisting mode is a general idea of the first order sliding mode. It is based on derivation with higher order for the sliding surface to reduce the chattering phenomena and ensure high robustness against disturbance. The super twisting algorithm convergence is insured around the origin of $(s, \dot{s})$ phase diagram. A general form of sliding-surface in the phase plane was proposed by Slotine and Li [24] as (12):

$$s = \left(\frac{d}{dt} + k_i \right)^{n-1} \cdot e(t) \tag{12}$$

where n is the system relative degree, e is the tracking error, and k is a positive constant that interprets the sliding surface dynamics. For autonomous vehicle path-following, the control law design depends mainly on two variable errors (y_{e1}, θ_{e1}). For that purpose, the proposed surface is designed to merge both the lateral error, y_{e1}, and the angular error, θ_{e1}, into one sliding-surface, as (13):

$$s_\psi = y_{e1} + k \cdot \theta_{e1} \tag{13}$$

By using (10), its corresponding derivative (14):

$$\dot{s_\psi} = v \cdot sin(\theta_{e1}) + (L_a \cdot cos(\theta_{e1}) + k) \cdot \left(v \cdot cos(\beta_R) \cdot \frac{tan(\psi_r+\beta_F) - tan(\beta_R)}{l} \right) \tag{14}$$

Based on [25] the super twisting control law for the steering controller can be expressed as (15):

$$\psi_{ST} = \psi_1 + \psi_2 \tag{15}$$

The first part ψ_1 ensures the convergence of the sliding surface to zero, and it is given as (16):

$$\dot{\psi_1} = -\beta_\psi \cdot sign(s_\psi) \tag{16}$$

While the second part allows to get soft response by ensuing $\dot{s_\psi} = 0$ as (17):

$$\psi_2 = -\lambda_\psi \cdot |s_\psi|^\rho \cdot sign(s_\psi) \tag{17}$$

Here, ρ is a positive coefficient used to adjust the degree of nonlinearity and it is defined by $0 < \rho \le 0.5$. This coefficient is mostly fixed at 0.5 to realize the maximum second order sliding mode control. While λ_ψ and β_ψ are positive gains for the super twisting controller, to satisfy the conditions that ensure the system convergence, these gains should be chosen as (18) and (19) [25]:

$$\beta_\psi > \frac{\Phi_M}{\Gamma_M} \tag{18}$$

$$\lambda_\psi > \frac{4 \cdot \Phi \cdot \Gamma_M (\beta_\psi + \Phi)}{\Gamma_m{}^3 (\beta_\psi - \Phi)} \tag{19}$$

where Γ_M and Γ_m are the upper and lower bounds of the uncertain function Γ, and Φ_M is the upper bound of the uncertain function Φ. These quantities are positive terms which can be defined at the second derivative sliding manifold (20):

$$\ddot{s_\psi} = \Phi(x, t) + \Gamma(x, t) \cdot \dot{\psi} \tag{20}$$

The second derivative of the sliding surface is derived as (21):

$$\ddot{s_\psi} = \frac{v \cdot cos(\beta_R) \cdot (L_a \cdot cos\theta_{e1} + k)}{l \cdot cos^2(\psi_r + \beta_F)} \dot{\psi} + v \cdot \dot{\theta}_{e1} \cdot cos\theta_{e1} - L_a \cdot \dot{\theta}_{e1}{}^2 \cdot sin\theta_{e1} \tag{21}$$

Which gives (22) and (23):

$$\Gamma = \frac{v \cdot cos(\beta_R) \cdot (L_a \cdot cos\theta_{e1} + k)}{l \cdot cos^2(\psi_r + \beta_F)} \tag{22}$$

$$\Phi = v \cdot \dot{\theta}_{e1} \cdot cos\theta_{e1} - L_a \cdot \dot{\theta}_{e1}{}^2 \cdot sin\theta_{e1} \tag{23}$$

Hence, the desired steering angle, representing the control law of the system, is deduced as (24):

$$\psi_d = -\lambda_\psi \cdot |s_\psi|^{0.5} \cdot sign(s_\psi) - \int \beta_\psi \cdot sign(s_\psi) dt \tag{24}$$

To guarantee the system stability, a positive definite Lyapunov function must be chosen for the system state variables, and then its derivative must be negative semi-definite. The Lyapunov candidate is defined based on [26] as (25):

$$V = \beta_\psi \cdot |s_\psi| + \frac{1}{2} \cdot \psi_1{}^2 \tag{25}$$

The nonlinear state model defined in (1) can be simplified based on a small degree assumption of side-slip angles as (26):

$$\begin{bmatrix} \dot{x}_r \\ \dot{y}_r \\ \dot{\theta}_r \end{bmatrix} = v \cdot \begin{bmatrix} \cos(\theta_r) \\ \sin(\theta_r) \\ \frac{\tan(\psi_r)}{l} \end{bmatrix} + P \tag{26}$$

where P denotes the system perturbation (27):

$$P = v \cdot \begin{bmatrix} 0 & -\sin(\theta_r) \\ 0 & \cos(\theta_r) \\ \frac{1}{l.\cos^2\psi_r} & -\frac{1}{l} \end{bmatrix} \cdot \begin{bmatrix} \beta_F \\ \beta_R \end{bmatrix} \tag{27}$$

Assuming that the system perturbation P is bounded with a known constant $G > 0$ as (28):

$$P \leq G. \left| s_\psi \right|^{0.5} \tag{28}$$

Thus, the derivative of V can be written as (29):

$$\dot{V} \leq \beta_\psi. sign(s_\psi). \left(-\lambda_\psi. \left| s_\psi \right|^{0.5}. sign(s_\psi) + G. \left| s_\psi \right|^{0.5} \right) \tag{29}$$

By choosing $\lambda_\psi > G$, the gradient is negative semi-definite right-hand side. Then, the asymptotic stability of the system is ensured.

4. VEHICLE VELOCITY PLANNING

In this section, an approach for adapting the vehicle velocity with trajectory curvatures by generating a speed profile to tune an ideal performance respecting human comfort is developed. The vehicle velocity may depend on several factors like road nature, natural factors, and road speed limits, which can be realized by applying a simple conditional statement. However, the most important factor is the path geometry; this last factor will be the focus of our research.

An overall workflow of vehicle trajectory-tracking using speed planning is presented in Figure 2. Depending on the trajectory coordinates, information about the sharp curves in the path could be extracted; then, by using this information, the optimal velocity for each sharp curve is computed. The generated speed profile is then included in the control law formula to compute the required steering angle, ensuring smooth vehicle navigation with minimum distance error.
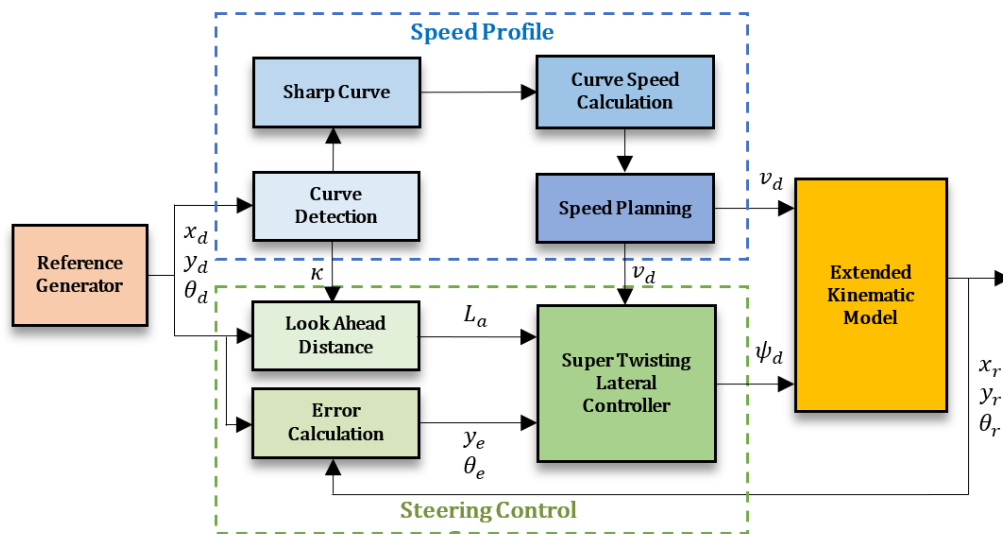

Figure 2. Path tracking structure using speed profile generation

4.1. Curve identification

The identification of sharp curves in a trajectory is a main factor in speed adaption procedures. A crucial step in this identification can be performed by computing the bearing-angle. The bearing-angle equation through three consecutive points A, B, and C is presented as (30) [27]:

$$\alpha = \cos^{-1}\left(\frac{(x_B-x_A)(x_C-x_B)-(y_B-y_A)(y_C-y_B)}{\sqrt{(x_B-x_A)^2+(x_C-x_B)^2}\cdot\sqrt{(y_B-y_A)^2+(y_C-y_B)^2}}\right)\cdot\frac{180}{\pi} \tag{30}$$

where (x_A, y_A), (x_B, y_B) and (x_C, y_C) are the coordinates of the points A, B, and C, respectively.

The bearing-angle is used to define the direction of one-point relative to another point. Once the bearing-angle is computed, a threshold value needs to be fixed for precise identification of curves. In this paper, a value of $5°$ is used. When the computed bearing-angle is greater than or equal the threshold value, a new curve begins, and it is identified by its curvature point (PC), or the current curve does not end yet. While in the case when the computed bearing-angle is less than or equal to the threshold value, then the exiting curve ends and is identified by its tangency point (PT) [28]. Once the trajectory curves are identified with their curvature points and tangency points, then the curves main characteristics can be extracted from Figure 3. In the figure, the radius, the intersection point, the curve center, the curve length, the central angle, and the length chord are symbolized by (R), (PI), (O), (L), (γ), and (C) respectively [29].
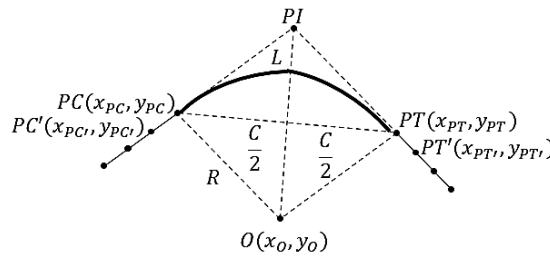

Figure 3. Curve parameters

Based on Figure 3 the curve main parameters are computed using these (31)-(34):

$$R = \sqrt{(x_{PC} - x_O)^2 + (y_{PC} - y_O)^2} \tag{31}$$

$$C = \sqrt{(x_{PT} - x_{PC})^2 + (y_{PT} - y_{PC})^2} \tag{32}$$

$$\gamma = 2\cdot\sin^{-1}\left(\frac{C}{2R}\right)\cdot\frac{180}{\pi} \tag{33}$$

$$L = \frac{\gamma.\pi}{180}\cdot R \tag{34}$$

4.2. Speed planning algorithm

Working on minimizing the error vector when the autonomous vehicle is navigating through the trajectory, a speed-planning algorithm is required to control the vehicle speed against lane constraints. By using the information of trajectory curves, friction coefficient, and super-elevation angle, a speed profile can be generated to ensure smooth motion with minimum distance error [30]. According to Figure 4 the centrifugal force is applied to the vehicle as (35):

$$F_c = m.\frac{v^2}{R} \tag{35}$$

From the net forces applied in the horizontal and vertical directions, the centrifugal and normal forces can be expressed by (36) and (37) as:

$$F_c = N\cdot\sin(\sigma) + N\cdot\mu\cdot\cos(\sigma) \tag{36}$$

$$N = \frac{m\cdot g}{\cos(\sigma)-\mu\cdot\sin(\sigma)} \tag{37}$$

where g is the gravitational acceleration, μ is the friction coefficient, and σ is the bank angle.

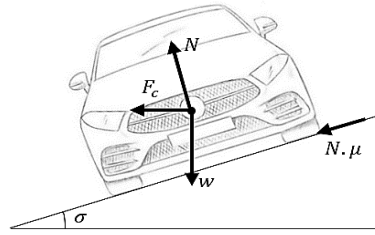

Figure 4. Forces applied to the vehicle

Then by using (35), (36), and (37), we get (38):

$$\frac{\tan(\sigma)+\mu}{1-\mu\cdot\tan(\sigma)}\cdot g = \frac{v^2}{R} \tag{38}$$

By defining the curvature $\kappa = \frac{1}{R}$ and the super-elevation $\vartheta = \tan(\sigma)$, the vehicle speed can be defined by (39):

$$v = \sqrt{\frac{(\vartheta+\mu)\cdot g}{(1-\mu\cdot p)\cdot \kappa}} \tag{39}$$

The friction coefficient is limited from 0.1 to 0.16 while the super-elevation is between 6% and 8% [30]. In real situation, the driver changes the speed depending on the trajectory curvatures. The required distance, d, between two speed values depends mainly on the vehicle actual speed, the desired speed, and the acceleration value as expressed in (40):

$$d = \frac{v_d^2 - v_a^2}{2\cdot a} \tag{40}$$

where v_d is the desired speed, v_a is the actual speed, and a is the required acceleration value.

5. RESULTS AND DUSCUSSION

In this section, we present simulation results of the proposed speed planning algorithm with super twisting control technique. To ensure applying our method to different kinds of situations, two proposed trajectories with distinct profiles and curve features are considered with the aim of showing the performance enhancement of the tracking accuracy through varied circumstances. The first trajectory has four sharp curves with a total distance of $2.3\ Km$, while the second has six sharp curves with a total distance of $3.5\ Km$ as shown in Figure 5. The vehicle starts motion from a starting point at the coordinate $(0,0)$ and navigates anticlockwise until reaching the ending point at the same coordinates as the starting point.
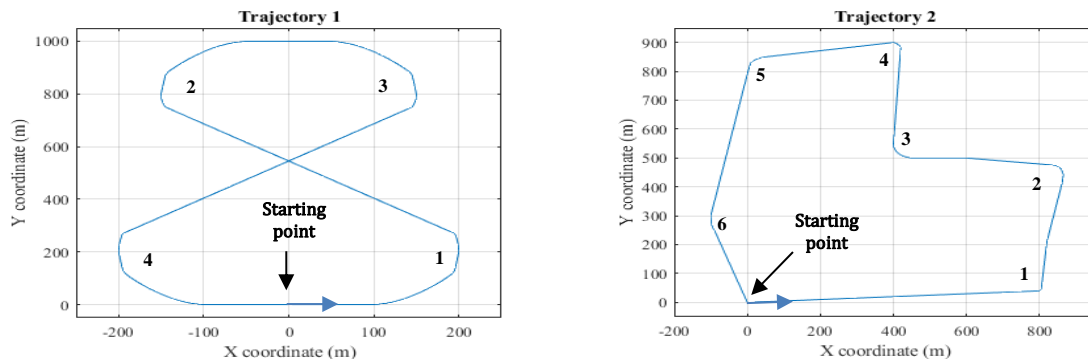

Figure 5. Vehicle tracking trajectories

5.1. Results using constant velocity

The vehicle navigation performance through the desired trajectories using constant velocity profile is presented in this section. The vehicle starts motion with initial velocity of $0\ m/s$; respecting the vehicle acceleration for passenger comfort, the vehicle velocity increases to reach a maximum value of $16.67\ m/s$. Figure 6 demonstrates the lateral and orientation errors results. As can be seen from this figure, the super twisting controller makes the vehicle to pursuit the reference trajectory with small errors. The observed peaks in some parts are mainly corresponding to the trajectories curvatures shown in Figure 5, where the vehicle started turning, to quickly adjusted back to the safety boundaries.

Figure 7 presents the steering angle command and yaw rate during the trajectory-tracking task. It is obvious that the vehicle autonomously drives around the testing place for multiple rounds and throughout the simulation process. The use of super twisting controllers results a smooth steering angle changing curve that does not seem to shudder a lot.
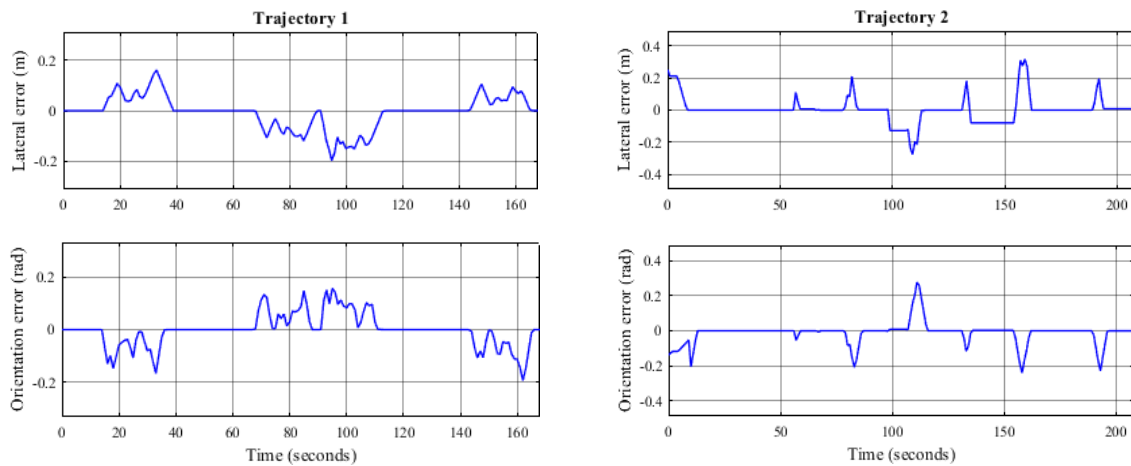
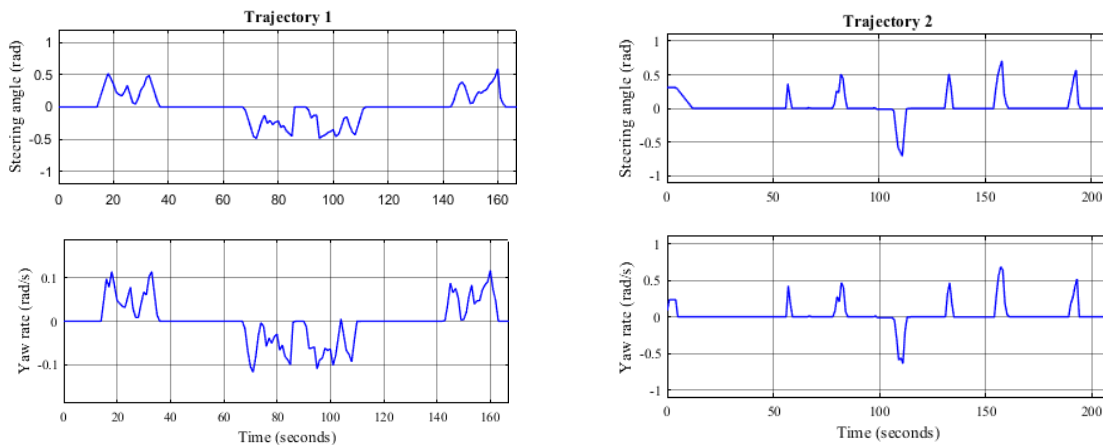Figure 6. Lateral and orientation errors using constant velocity

Figure 7. Steering angle and yaw rate using constant velocity

5.2. Results using velocity planning

This section presents the vehicle navigation performance through the desired trajectories using speed-planning algorithm. The speed of the vehicle is limited with a maximum value of $16.67\ m/s$. Figure 8 presents the generated speed profile, lateral and orientation errors for vehicle trajectory-tracking. Depending on trajectory curvatures, the speed-planning algorithm generates an adequate speed profile for vehicle travel to ensure smooth tracking with high precision. From this figure, it is remarkable that the lateral and orientation errors obtained from merging the speed-planning algorithm with super twisting controller are lower than the ones obtained from using super twisting controller with constant velocity. The speed-planning algorithm works to decrease the vehicle velocity in sharp curves, and that offers the possibility to track the real trajectory with more accuracy.
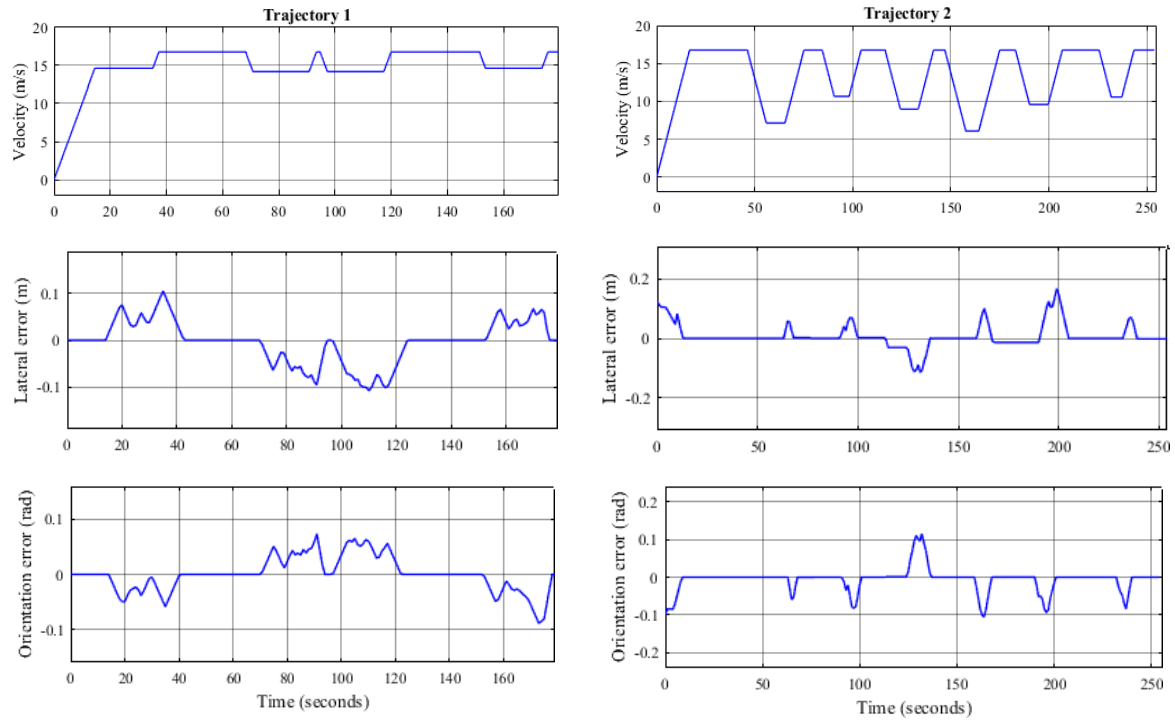
Figure 8. Speed profile, lateral and orientation errors using speed-planning

Figure 9 presents the vehicle steering angle and yaw rate during its navigation through the desired trajectories. The speed-planning algorithm generates an ideal speed that is used in the lateral control to provide a steering angle to be applied by the vehicle steering wheel. Including this speed profile in steering angle control provides large impact in generating an appropriate command that offers smooth tracking. Figure 10 summarizes the comparison results of vehicle navigation errors with and without using the speed-planning algorithm. The lateral R.M.S error is reduced by 42.86% and 45.45%, while the orientation r.m.s error is reduced by 57.14% and 44.44% for trajectory 1 and 2, respectively. The reduction of these errors proves the high performance of the speed-planning algorithm with super twisting controller and its role in providing good trajectory-tracking with small error.
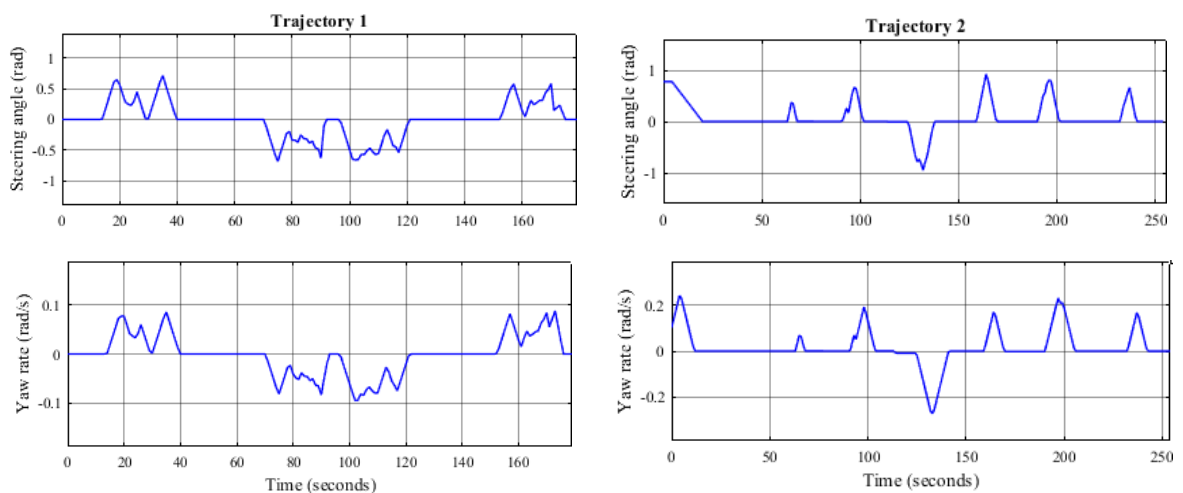
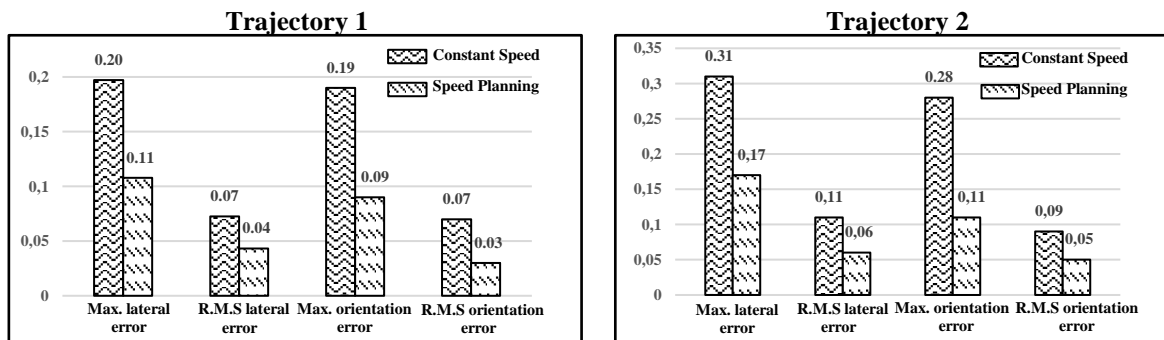Figure 9. Steering angle and yaw rate using speed-planning

Figure 10. Average errors

6. CONCLUSION

In this work, we have presented a performance enhancement for autonomous vehicle trajectory tracking by combining a designed speed-planning algorithm with lateral super twisting control. The main characteristics of trajectory curves were used to extract the ideal speed of each part of the trajectory and then obtain a perfect speed profile for vehicle navigation. Then, a super twisting controller was designed to control the vehicle lateral motion and ensure smooth tracking with high performance. The system stability with super twisting control was proved mathematically using Lyapunov theory. The obtained results through different kinds of scenarios proved that the designed control algorithm is capable of tracking the defined trajectory with high accuracy and effectiveness. The importance of including the speed-planning was illustrated by decreasing the error value and ensuring comfortable motion through the whole trajectory.

REFERENCES

[1]   A. Alsalman, L. N. Assi, S. Ghotbi, S. Ghahari, and A. Shubbar, "Users, planners, and governments perspectives: A public survey on autonomous vehicles future advancements," *Transportation Engineering*, vol. 3, pp. 1–14, Mar. 2021, doi: 10.1016/j.treng.2020.100044.
[2]   S. Dixit *et al.*, "Trajectory planning and tracking for autonomous overtaking: State-of-the-art and future prospects," *Annual Reviews in Control*, vol. 45, pp. 76–86, 2018, doi: 10.1016/j.arcontrol.2018.02.001.
[3]   N. H. Amer, H. Zamzuri, K. Hudha, and Z. A. Kadir, "Modelling and control strategies in path tracking control for autonomous ground vehicles: A review of state of the art and challenges," *J. of Intel & Rob. Syst.* vol. 86, pp. 225–254, 2017, doi: 10.1007/s10846-016-0442-0.
[4]   S. Bacha, M. Y. Ayad, R. Saadi, A. Aboubou, M. Bahri, and M. Becherif, "Modeling and control technics for autonomous electric and hybrid vehicles path following," in *2017 5th International Conference on Electrical Engineering-Boumerdes (ICEE-B)*, Oct. 2017, pp. 1–12. doi: 10.1109/ICEE-B.2017.8191998.
[5]   E. Lucet, R. Lenain, and C. Grand, "Dynamic path tracking control of a vehicle on slippery terrain," *Control Engineering Practice*, vol. 42, pp. 60–73, Sep. 2015, doi: 10.1016/j.conengprac.2015.05.008.
[6]   M. Deremetz, R. Lenain, and B. Thuilot, "Path tracking of a two-wheel steering mobile robot: An accurate and robust multi-model off-road steering strategy," in *2018 IEEE International Conf. on Rob. and Auto.*, 2018, pp. 3037–3044. doi: 10.1109/ICRA.2018.8460598.
[7]   W. Zhang, "A robust lateral tracking control strategy for autonomous driving vehicles," *Mechanical Systems and Signal Processing*, vol. 150, pp. 1–15, Mar. 2021, doi: 10.1016/j.ymssp.2020.107238.
[8]   A. Mohammadzadeh and H. Taghavifar, "A robust fuzzy control approach for path-following control of autonomous vehicles," *Soft Computing*, vol. 24, no. 5, pp. 3223–3235, Mar. 2020, doi: 10.1007/s00500-019-04082-4.
[9]   X. Ji, X. He, C. Lv, Y. Liu, and J. Wu, "Adaptive-neural-network-based robust lateral motion control for autonomous vehicle at driving limits," *Control Engineering Practice*, vol. 76, pp. 41–53, Jul. 2018, doi: 10.1016/j.conengprac.2018.04.007.
[10]   K. Akermi, S. Chouraqui, and B. Boudaa, "Novel SMC control design for path following of autonomous vehicles with uncertainties and mismatched disturbances," *Int. J. of Dyn. and Con.*, vol. 8, pp. 254–268, 2020, doi: 10.1007/s40435-018-0478-z.
[11]   J. Guo, Y. Luo, and K. Li, "Robust H∞ fault-tolerant lateral control of four-wheel-steering autonomous vehicles," *International Journal of Automotive Technology*, vol. 21, no. 4, pp. 993–1000, Aug. 2020, doi: 10.1007/s12239-020-0094-8.
[12]   A. A. Baker and Y. Y. Ghadi, "Autonomous system to control a mobile robot," *Bulletin of Electrical Engineering and Informatics*, vol. 9, no. 4, pp. 1711–1717, Aug. 2020, doi: 10.11591/eei.v9i4.2380.
[13]   P. N. F. M. Shamsuddin, R. M. Ramli, and M. A. Mansor, "Navigation and motion control techniques for surface unmanned vehicle and autonomous ground vehicle: a review," *Bulletin of Electrical Engineering and Informatics*, vol. 10, no. 4, pp. 1893–1904, Aug. 2021, doi: 10.11591/eei.v10i4.3086.
[14]   C. G. Serna and Y. Ruichek, "Dynamic speed adaptation for path tracking based on curvature information and speed limits," *Sensors*, vol. 17, no. 6, p. 1383, Jun. 2017, doi: 10.3390/s17061383.
[15]   S. Thrun *et al.*, "Stanley: The robot that won the DARPA grand challenge," *Journal of Field Robotics*, vol. 23, no. 9, pp. 661–692, Sep. 2006, doi: 10.1002/rob.20147.
[16]   J. Taheri-Kalani and N. Zarei, "An adaptive technique for trajectory tracking control of a wheeled mobile robots without velocity measurements," *Automatic Control and Computer Sciences*, vol. 50, no. 6, pp. 441–452, 2016, doi: 10.3103/S0146411616060080.
[17]   J.-W. Lee and S. Prabhuswamy, "A unified framework of adaptive cruise control for speed limit follower and curve speed control function," in *SAE Technical Papers*, Apr. 2013, pp. 1–8. doi: 10.4271/2013-01-0618.
[18]   Z. Deng, D. Chu, C. Wu, Y. He, and J. Cui, "Curve safe speed model considering driving style based on driver behaviour questionnaire," *Trans. Res. Part F: Traffic Psyc. and Behaviour*, vol. 65, pp. 536–547, 2019, doi: 10.1016/j.trf.2018.02.007.
[19]   R. Rajamani, *Vehicle dynamics and control*, 2nd ed. New York: Springer, 2012, doi: 10.1007/978-1-4614-1433-9_2.

[20] R. Siegwart, I. R. Nourbakhsh, and D. Scaramuzza, "Mobile robot kinematics," in *Introduction to Autonomous Mobile Robots*, 2nd ed., London: MIT Press, 2011, pp. 57–99.

[21] A. Guillet, R. Lenain, B. Thuilot, and P. Martinet, "Adaptable robot formation control: Adaptive and predictive formation control of autonomous vehicles," *IEEE Robotics & Auto. Magazine*, vol. 21, no. 1, pp. 28–39, 2014, doi: 10.1109/MRA.2013.2295946.

[22] R. Lenain, M. Deremetz, J.-B. Braconnier, B. Thuilot, and V. Rousseau, "Robust sideslip angles observer for accurate off-road path tracking control," *Advanced Robotics*, vol. 31, no. 9, pp. 453–467, May 2017, doi: 10.1080/01691864.2017.1280414.

[23] C. Cariou, R. Lenain, B. Thuilot, and M. Berducat, "Automatic guidance of a four-wheel-steering mobile robot for accurate field operations," *Journal of Field Robotics*, vol. 26, no. 6–7, pp. 504–518, Jun. 2009, doi: 10.1002/rob.20282.

[24] J.-J. E. Slotine and W. Li, "Sliding control," in *Applied Nonlinear Control*, Englewood Cliffs: Prentice hall, 1991, pp. 276–310.

[25] A. Levant, "Higher-order sliding modes, differentiation and output-feedback control," *International Journal of Control*, vol. 76, no. 9–10, pp. 924–941, Jan. 2003, doi: 10.1080/0020717031000099029.

[26] A. Barth, M. Reichhartinger, J. Reger, M. Horn, and K. Wulff, "Lyapunov-design for a super-twisting sliding-mode controller using the certainty-equivalence principle," *IFAC-PapersOnLine*, vol. 48, no. 11, pp. 860–865, 2015, doi: 10.1016/j.ifacol.2015.09.298.

[27] Z. Li, M. V. Chitturi, A. R. Bill, and D. A. Noyce, "Automated identification and extraction of horizontal curve information from geographic information system roadway maps," *Transportation Research Record: Journal of the Transportation Research Board*, vol. 2291, no. 1, pp. 80–92, Jan. 2012, doi: 10.3141/2291-10.

[28] W. Luo and L. Li, "Automatic geometry measurement for curved ramps using inertial measurement unit and 3D LiDAR system," *Automation in Construction*, vol. 94, pp. 214–232, Oct. 2018, doi: 10.1016/j.autcon.2018.07.004.

[29] S. Gargoum, K. El-Basyouny, and J. Sabbagh, "Automated extraction of horizontal curve attributes using LiDAR data," *Transportation Research Record: Journal of the Transportation Research Board*, vol. 2672, no. 39, pp. 98–106, 2018, doi: 10.1177/0361198118758685.

[30] M. Park, S. Lee, and W. Han, "Development of steering control system for autonomous vehicle using geometry-based path tracking algorithm," *ETRI Journal*, vol. 37, no. 3, pp. 617–625, Jun. 2015, doi: 10.4218/etrij.15.0114.0123.

BIOGRAPHIES OF AUTHORS

Sofiane Bacha obtained the BSc degree in electrical and electronic engineering and Master diploma in control engineering from the instute of electrical and electronic engineering in Boumerdes University, in 2014 and 2016 respectively. He is currently working toward the PhD degree from the department of electrical engineering in the University of Biskra and he is a member in the Energy Systems Modeling Laboratory. His research interests are in the fields of electric vehicle, autonomous vehicle, energy mangement, control system, modeling and electric machine. He can be contacted at email: sofiane.bacha@hotmail.fr.

Ramzi Saadi received the BSc and Master diploma and the PhD degree in electrical engineering from the University of Biskra, in 2008, 2010 and 2015 respectively. Mr. Saadi is an Associate professor with the University of Biskra since 2015 and he is a member in the Energy Systems Modeling Laboratory. Actually, he is the head of the department of electrical engineering in the University of Biskra. His research interests are related to renewable energies; fuel cell, energy management, electric vehicle, autonomous vehicle and DC/DC converter. He can be contacted at email: r.saadi@univ-biskra.dz.

Mohamed-Yacine Ayad obtained the MSc and PhD degrees in Electrical Engineering from ENSEM-INPL, France in 1999 and 2004. From 2004 to 2007, he was working as research assistant at the University of Technology at Belfort and Montbéliard (UTBM), France. Since 2007, he has been working as R&D in Hybrid Vehicle Industrial Applications. Currently, he is International Responsible of Development at Groupe PSA, France. His main research is in the field of power electronics, modelling, nonlinear control and energy management in embedded, smart and micro grids systems applications using battery, supercapacitor, fuel cell, WDG and PV sources. He can be contacted at email: ayadmy@gmail.com.

Abdennacer Aboubou obtained his engineering degree in 1986 and his degree of Magister in Electrical machinery from the University of Annaba in Algeria. He was a Lecturer in University of Annaba in 1988, in University of Batna in 1994 and in University of Biskra in 1996. He received his PhD degree in Electrical machinery from University of Biskra, in 2005. Currently he is in the Laboratory of Energy Systems Modelling and he collaborating with the Fuel Cell Institute (FCLab), France and with GREPCI the Research Group in Power Electronics and Industrial Control in Montreal, Canada. His research interests are in the fields of modelling, nonlinear control, energy management of hybrid systems, reliability and optimization of energy transport systems. A. Aboubou is a reviewer in the IEEE review (transactions on energy conversion) and ELSEVIER (control engineering & practice). He can be contacted at email: aboubou.nacer@gmail.com.